Chapter V

Studies on Vesicular Aggregates of Dimethyldioctadecylammonium Bromide (DDOAB): Influence of Cosurfactants and Hydroxyaromatic Dopants

5.1. Introduction and review of previous works

Vesicles are amphiphile aggregates with closed bilayered structures similar to those of the lamellar phase characterized by two distinct water compartments, one forming the core and other the external medium. Vesicles find major applications in the field of drug delivery, nanotechnology and two-dimensional-crystallization of proteins as has already been discussed [1]. Much of the interesting physical chemistry of vesicles and liposomes has been established from studies of lipids, either from the natural sources or synthesized as pure lipids. However, the field has been greatly extended with the development of synthetic surfactants capable of mimicking the membrane forming lipids [2]. While the architecture of these artificial membranes is considerably simpler than that of cell membranes, they possess some common characteristics of the natural membranes with respect to permeability, chain melting temperature and like natural membranes they are capable of accommodating small proteins and natural polymers [3, 4].

Dimethyldioctadecylammonium bromide (DDOAB) is a synthetic surfactant which, in excess of water, forms structures capable of mimicking the biological membranes. DDOAB is a long (C_{18}) double tailed cationic surfactant that self assemble spontaneously into giant closed bilayered structures above the gel-to-liquid crystalline phase transition temperature, T_m (~ 45°C) at low concentration conditions (1.0 mM) [5-9]. In general, the transition temperature T_m of vesicle is a function of the preparation method. Sometimes, bath or probe sonication is used to prepare small unilamellar vesicle while slow injection of chloroform results in

large vesicle formation [10,11]. In a recent protocol, the dichloromethane injection formed stable large unilamellar vesicles from dimethyldioctadecylammonium chloride (DDOAC). Of the several methods used for vesicle preparation, the hot water method has following advantages: the measured properties are better reproducible and that the preparation conditions such as temperature and concentration can be well controlled.

The solubilisation of vesicles by micelle forming surfactants is important as far as elucidation and control of biological membrane component reconstruction are concerned. The overall process of solubilisation is one of vesicle-to-micelle transition. This liquid crystalline to micellar phase transition has been successfully explained by the Lichtenberg three stage model [12]. The changes that occur at each of the stages mainly depend on the surfactant-to-lipid molar ratios. When this ratio is small, the surfactant monomers are not instrumental in causing any major structural changes to the lipid bilayer. However, at certain surfactant/lipid molar ratio the bilayer gets saturated and the process of vesicle disintegration is initiated. On further increasing the molar ratio, a complete solubilisation takes place resulting in the formation of only mixed micelles and the surfactant micelles. The most extensively studied system is the solubilisation of phospholipids by non-ionic surfactants viz; Triton X-100, octylglucoside (OG), $C_{12}E_8$ and related polyoxyethylene glycol (PEG) [13-16]. The reason is obvious. The phospholipids along with sterols make up about half the mass of biological membranes and the structure and properties of the bilayers are relatively well characterised. Other lipids, although present in relatively small quantities, play crucial roles as enzyme cofactors, electron carriers, light-absorbing pigments and intracellular messengers [17].

In general, nonionic surfactants exhibit less negative side effects than ionic surfactants [18]. Studies on the interaction of uncharged surfactants with vesicles have, therefore, been investigated extensively during the last two decades [19-22]. Tween 20 is a polysorbate surfactant whose stability and relative non-toxicity favour its use as a detergent and emulsifier in a number of domestic, scientific, and pharmacological applications. Keeping the above in view the interaction of non-ionic micelle forming surfactant Tween 20 with spontaneously formed vesicle

dispersions of DDOAB are studied. The original approach, which is still popular [23-25], defines the saturation point as the surfactant/lipid molar ratio where light scattering starts to decrease and the solubilisation point as the surfactant/lipid molar ratio where further lowering of light scattering stops. However, one should not rely on these methods alone, as the transition points are hardly detectable with sufficient accuracy. Hence, values corresponding to the transition points should be determined by more than one independent methods. Therefore, in the present work three independent methods, viz., DSC, turbidity and fluorescence anisotropy measurements have been applied to determine the effective surfactant/lipid ratio producing saturation and solubilisation.

In the second part of the chapter, the effect of alkyltrimethylammonium bromides and alkylpyridinium halides on the thermal stability of DDOAB vesicle solutions have been investigated by DSC studies on solutions containing fixed concentrations of DDOAB to which had been added varying concentrations of the additives. In general anionics increase, nonionics and zwitterionics decrease the T_m of DDOAB [26-28]. The cationic surfactants, however, may increase, decrease or leave the T_m unchanged [29,30]. For example Blandamer et. al. have shown, using DSC, that the addition of CTAB and SDS decreases and increases the T_m of DDOAB respectively [31]. According to these authors the major reason for the thermal stability of the vesicle were due to the influence of the charged head groups of CTAB and SDS and not necessarily a consequence of simply the length of the alkyl chains of the surfactants. In a more generalized study Kacperska reported the effect of alkyltrimethylammonium bromides (C_nTAB: n ranging from C_{12}-C_{18}) on the T_m of DDOAB in aqueous solution and found that the lower members of the surfactants were not influential in decreasing the T_m to a greater extent and that $C_{18}TAB$, having similar chain length as that of the vesicle bilayer, enhances the T_m [29]. The study clearly depicts the role of the alkyl chains of surfactants in producing changes in T_m. A similar study using the same set of surfactants and the vesicle has been performed recently by Aves et. al. [32]. There are no reports on the effect of alkylpyridinium halides on the T_m of DDOAB system. In the quaternary cationics, pyridinium compounds have smaller cmc's than the corresponding trimethylammonium compound due to their planar

headgroups. Therefore, it would be interesting to compare the effects of the two quaternary cationics on the phase transition of DDOAB. In the last part of this chapter, the effects of hydroxyaromatic compounds viz., 1-naphthol, 2-naphthol, 2,3-dihydroxynaphthalene and 2,7-dihydroxynaphthalene on the gel-to-liquid crystalline phase transition temperature of DDOAB have been investigated.

In spite of being one of the most investigated vesicle-forming cationic synthetic amphiphiles, the structure and properties of dioctadecyldimethyl ammonium bromide vesicles alone or in combination with other additives is still not fully understood. Since DODAB is one typical example of the bilayer forming double-chained cationic surfactants that often behave similarly to biomembrane lipids in an aqueous environment [33], better understanding is warranted. Therefore, the present investigation has been carried out with an aim to better insight of the present understanding of the phase transition properties of biological membranes. Values of T_m reported here for DODAB in presence of CPC or CPB may be useful to those who make practical or scientific use of these synthetic vesicles in particular and of amphiphilic vesicles in general.

5.2. Gel-to-liquid crystalline phase transition temperature.

One of the most striking properties of vesicle-forming surfactants in solution, such as the cationic quaternary ammonium series of the double chain dialkyldimethylammonium bromide is the gel to liquid-crystalline phase transition (or melting) temperature (T_m). Since the vesicles are prepared above this critical temperature, this property is usually used as the "finger print", or quality control for the so prepared vesicle dispersions [34-37]. Below T_m, the surfactants are poorly soluble in water and thus cannot at least spontaneously assemble as vesicles. Once prepared in the liquid-crystalline phase (i.e., above T_m), the vesicles remain stable for months even when stored in the gel phase, or below T_m [38,39]. There is, however, a lower temperature point below which the vesicles are destabilized [34].

In biological membranes, the phase transition temperature is very important for ensuring that the membrane has the correct fluidity and permeability for its particular application. Increasing alkyl chain length increases the transition temperature, while possession of unsaturated alkyl chains causes a decrease in transition temperature.

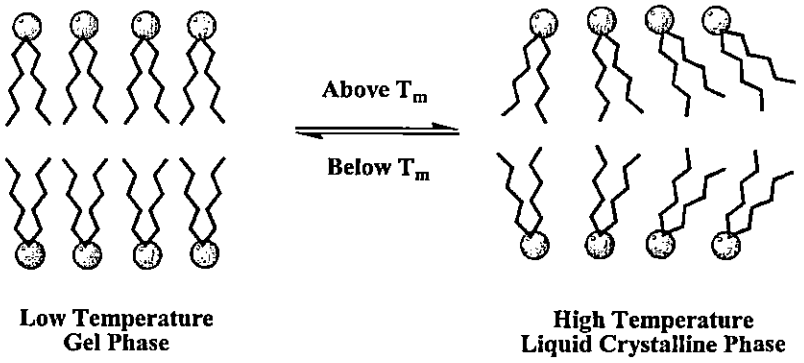

Figure 5.1. The gel-to-liquid crystalline phase transition.

Figure 5.1 shows the schematic representation, in aqueous solution, of a double tailed vesicle forming surfactant both in the gel and the liquid crystalline phase. At low temperatures the di-alkyl chains pack in an ordered fashion but with increasing temperature the vesicle undergo a gel-to-liquid crystalline phase transition (less ordered) at melting temperature T_m, which is a characterstics of the system. Using ^{1}H-nuclear magnetic resonance (^{1}H-NMR) spectroscopy, the surfactant fraction in the liquid-crystalline state can be determined [40].

5.3. Materials and Methods.

Dimethyldioctadecylammonium bromide with purity greater than 99% was used as received from Acros Organics (Belgium). Tween 20 (Puris grade) was procured from Sigma (USA) and used without further purification. Trans, trans, trans-1, 6-diphenyl-hexatriene, DPH (Aldrich product, USA) was recrystallised twice from acetone before use. Double distilled water was used throughout. The molecular structures of Tween 20, DPH and DDOAB are shown in figure 5.2.

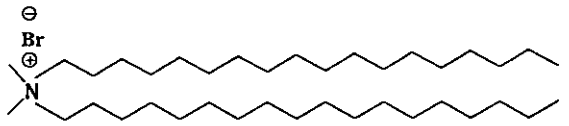

Dimethyldioctadecylammonium bromide (DDOAB)

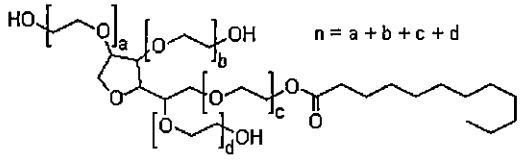

Polyoxyethylene Sorbitan Monolaurate (Tween-20)

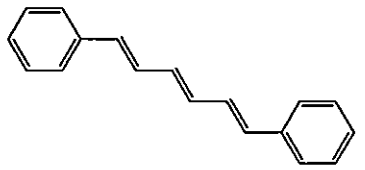

Trans, trans, trans-1, 6-diphenyl hexatriene (DPH)

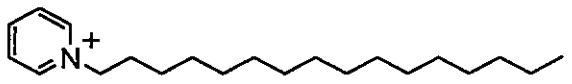

Hexadecylpyridinium ion

Figure 5.2. Molecular structures of DDOAB, Tween 20, DPH and Hexadecyl-pyridinium ion.

Sample preparation: Spontaneous DDOAB vesicle dispersions (stock solutions) were formed by simply dissolving the surfactant (5.0 mM) in water at ~ 60°C. The dispersions were then kept standing and cooled at room temperature and stored for 24 hours before the experiment. The stock solution was diluted to 1.0 mM for turbidity and fluorescence anisotropy studies. Mixed solutions of Tween 20/DDOAB were prepared by adding aliquots of 20mM aqueous Tween 20 in the vesicle dispersion to obtain the desired concentration.

Differential Scanning Calorimetric (DSC) Measurements: The DSC thermograms were obtained on a Perkin Elmer Pyris 6 DSC instrument, the temperature of which was raised at a constant rate of 1°C /min. The maximum of the main peak

corresponds to the gel-to-liquid crystalline phase transition temperature and the area under the peak measures the transition enthalpy. The data were analysed with the help of PYRIS software provided with the instrument. The DSC scans were repeated at least twice to check the reproducibility.

Fluorescence Anisotropy: The steady-state fluorescence anisotropy (r) measurements were performed on a Perkin Elmer LS-55 luminescence spectrophotometer equipped with a thermostating and magnetically stirred cell housing that allowed temperature control within ± 0.1 °C using a Thermo Neslab RTE-7 circulating water bath. The instrument is equipped with a polarization accessory, which uses the L-format instrumental configuration. Since DPH is insoluble in water, a 1.0 mM stock solution was prepared in 20 % (v/v) methanol-water mixture. The final concentration of the probe was adjusted to 2 μM by the addition of an appropriate amount of the stock solution. Before the measurement was made the solution had equilibrated for 10 minutes at a particular temperature. The sample was excited at 350 nm and the emission intensity was followed at 450 nm using excitation and emission slits with bandpass equal to 2.5 nm and 2.5-5.0 nm, respectively. A 430 nm cut-off filter was placed in the emission beam to reduce effects due to scattered radiation. The anisotropy measurements were carried out at different Tween 20/DDOAB mole ratios at 25 °C.

Turbidity and dynamic light scattering Measurements: The turbidity was monitored on a Jasco V530 spectrophotometer at a constant wavelength of 420 nm using a matched pair of quartz cell of 1 cm optical path length. The reference cell was filled with water for baseline control. The measurements were made 5 minutes after each addition of the Tween 20 solution in DDOAB dispersions. The temperatures of the cells were controlled using a thermostated water bath within ±0.1 °C. A Malvern 4700 light scattering apparatus with correlator (Malvern 7032) was used for dynamic light scattering measurements at a scattering angle of 90°, the temperature being 25°C. Results were based on an average of 15 measurements. Prior to analysis, the samples were filtered through a polysulfone filter (Whatman, 1 μmpore size) to prevent background scattering from dust contamination.

5.4. Results and discussions

5.4.1. Solubilisation of DDOAB vesicle by Tween 20

5.4.1.1. Differential Scanning Calorimetry (DSC)

Melting of lipids is an endothermic phenomenon; hence, DSC serves to be a useful tool to investigate the thermotropic phase behavior and to determine the T_m of amphiphiles in vesicles and liquid crystal systems [41-43]. The DSC thermogram of 5.0 mM nonsonicated pure DDOAB dispersion is shown in figure 5.3. Recent studies have shown that the T_m of 5.0 mM neat DDOAB is the same as that of the most often investigated 1.0 mM dispersion [44]. Moreover, an added advantage with the 5.0 mM dispersion is that the gel-to-liquid crystalline transition as well as the effect of other additives on the T_m is more pronounced [45]. Hence, a dispersion of 5.0 mM have been done for investigating T_m in the present study. The DDOAB dispersion was filled in the sample cell and the temperature was lowered to 15°C and kept at this temperature for about 5 min before making the upscan to 60°C under DSC. Two endothermic peaks at 36°C and 45.2°C respectively were observed and this is consistent with the previous reports on non sonicated DDOB vesicle dispersion [46,47] . On cooling, the sample displays a single exothermic peak at 40°C. The DSC thermogram for 5.0 mM aqueous DDOAB during heating and cooling cycle is shown in figure 5.3. The peak at 45.2°C has been identified as the main gel-to-liquid crystalline phase transition temperature. On the other hand, the peak at 36°C, which could be observed only when the sample temperature was lowered below 15°C, has been assigned to the melting of the patches perturbed by the vesicle–vesicle interaction/aggregation [48]. The origin of the pre-transition either in lipid or synthetic amphiphile vesicles is not clear. It may be attributed either to changes in the chain conformations [49] or to structural transformations within the amphiphile head groups [50]. Blandamer et. al. [48] reported that the addition of ionic surfactants to a non-sonicated DODAB vesicle dispersion eliminates the pre-transition peak and linked it to intervesicular interactions. The presence of small fraction of Tween 20 (0.1 molar ratio) in aqueous DDOAB replaces the two extrema at 36°C and 45.2°C with a single transition peak at 44.4°C. Since the solutions of Tween 20 and DDOAB for

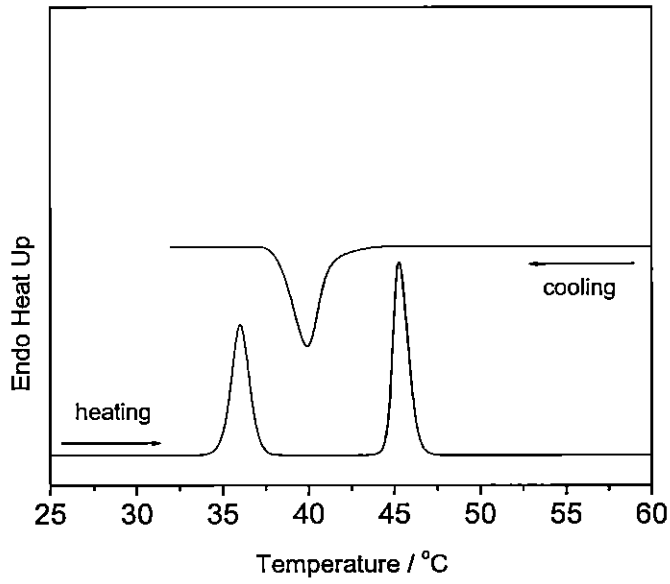

Figure 5.3. DSC thermogram of a 5 mM nonsonicated DDOAB dispersion during heating and cooling cycle. For clarity, the curves have been displaced on the heat capacity axis.

the DSC scan were prepared at room temperature, below the T_m of DDOAB, the overall system probably was not at equilibrium and therefore the first scan differed from the second scan. The system attains the meta stable state only after the completion of the first scan and that the penetration of Tween 20 surfactant into the bilayer occurs more rapidly in the liquid crystalline state. The second scan and all subsequent scans produced the same T_m and therefore, only the results from the second scans were considered. The DSC upscan thermogram of DDOAB for different Tween 20/DDOAB mole ratios, ranging from 0.1 to 4, are shown in figure 5.4 A.

With increasing concentration of Tween 20 the T_m of DDOAB dispersion shifts towards lower temperature. The hydrophobic interaction between the alkyl parts of the added surfactant and the vesicle allows the Tween 20 monomers to be partitioned in the vesicle phase thereby reducing the thermal stability of the more ordered gel state. Such a dramatic result could not have occurred if the Tween 20 molecules, instead of penetrating the bilayer, were located only in the aqueous phase between the vesicles. The presence of well defined peaks, upto Tween 20/DDOAB molar ratio of 1.5, indicates that the system is still rich in vesicles and

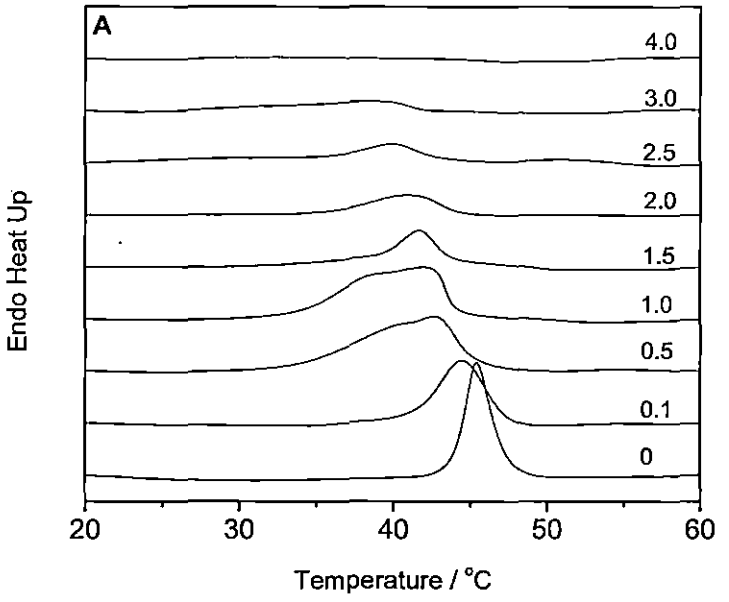

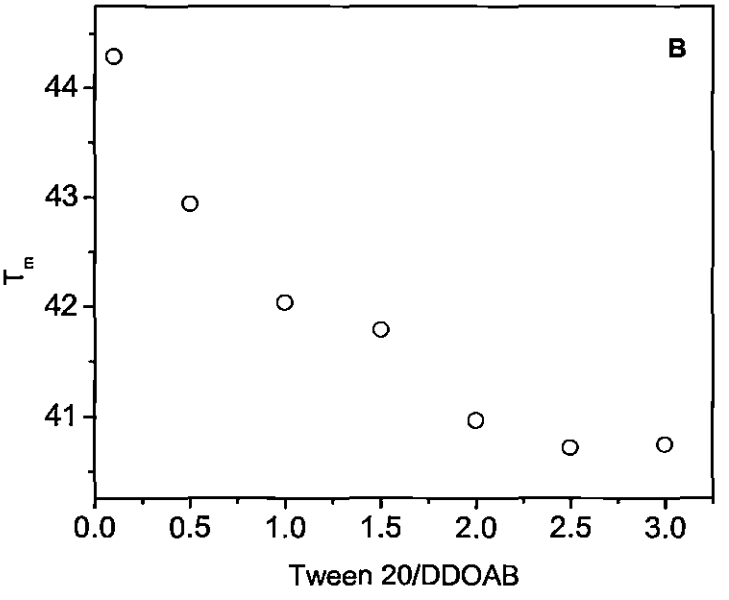

Figure 5.4. DSC upscans for 5 mM DDOAB dispersions at various Tween 20/DDOAB molar ratios (A). The Tween 20/DDOAB molar ratios are indicated in the figure. Curves have been offset from each other to avoid overlap. Figure B indicates the variation of Tm with Tween 20/DDOAB molar ratios.

that the saturation value is nearly 1.5. Further increase in the above molar ratio leads to lowering of T_m and more broadening of the peak that is associated with the gel-to-liquid crystalline phase transition temperature. The broadening of the transition peak would indicate that a two-phase gel to liquid crystalline region is crossed with each phase making a contribution to the enthalpy change (figure 5.4 A). This region most probably corresponds to the region where micelles and vesicles coexist. At still higher mole ratio the peak broadens considerably and ultimately disappear at around Tween 20/DDOAB ~ 4, indicating complete solubilisation of DDOAB vesicle dispersion. Once the complete solubilisation takes place, the system relaxes with mixed micelles only. The effect of Tween 20 surfactant on the phase transition temperature of DDOAB vesicle is shown in figure 5.4 B, where T_m is plotted as a function Tween 20/DDOAB mole ratio. The decreasing tendency of T_m with the addition of Tween 20 is clearly observable, especially at lower mole ratio regions. However, deviation from linearity is observed at higher mole ratio of the added surfactant. Similar lowering of T_m of DDOAB with concomitant broadening of the peaks has also been observed for Octaethylene Glycol n-Dodecyl Monoether ($C_{12}E_{18}$)/DDOAB ternary system where the DSC peak corresponding to complete solubilisation, disappears at the surfactant/lipid ratio of ~6 [51]. From the present study it seems apparent that Tween 20 is solubilising the vesicles formed by aqueous DDOAB system.

5.4.1.2. Turbidity and Dynamic Light Scattering Measurements

The impact of micelle forming surfactant on the vesicle/bilayer integrity can conveniently be followed by monitoring the turbidity of the vesicle dispersion at various surfactant/lipid molar ratios [52]. The plot of turbidity versus Tween 20/DDOAB molar ratio is shown in figure 5.5. For the present study, the turbidity is measured at a fixed wavelength of 300 nm with measurements made 5 min after subsequent addition of Tween 20 to DDOAB dispersion. At 300 nm, neither Tween 20 nor DDOAB have any absorption, therefore, any changes in this quantity are merely due to the scattering of light. There was a moderate increases in the turbidity upto a mole ratio of 0.68 and then it decreases until the mole ratio reaches

~5 and remains almost constant thereafter. The above mentioned two critical molar ratios, i.e., saturation and solubilisation, are shown in figure 5.5 by arrows. The initial increase in the turbidity upto mole ratio of 0.68 for the Tween 20/DDOAB system may be attributed to the increase in the size of the vesicle on account of the saturation of the vesicle bilayer with Tween 20 monomers. Further, the plot (figure 5.5) depicts a sharp fall in the turbidity after the saturation point due to partial rupturing of the DDOAB vesicle on account of the increase in the fraction of Tween 20 micelles in the vesicular system. This region (from molar ratio of 0.68 to 5) is, therefore, the region where vesicles and micelles coexist. Above Tween 20/DDOAB molar ratio of ~5 there is practically no change in the turbidity values indicating a complete vesicle to micelle transition to take place and that the system consists of mixed micelles only, as has already been mentioned. The results obtained in the present investigation are in accordance with the three stage model as predicted by Lichtenberg et. al. [12]. The values of the saturation and solubilisation molar ratios obtained by the turbidity and DSC measurements are in fair agreement with each other.

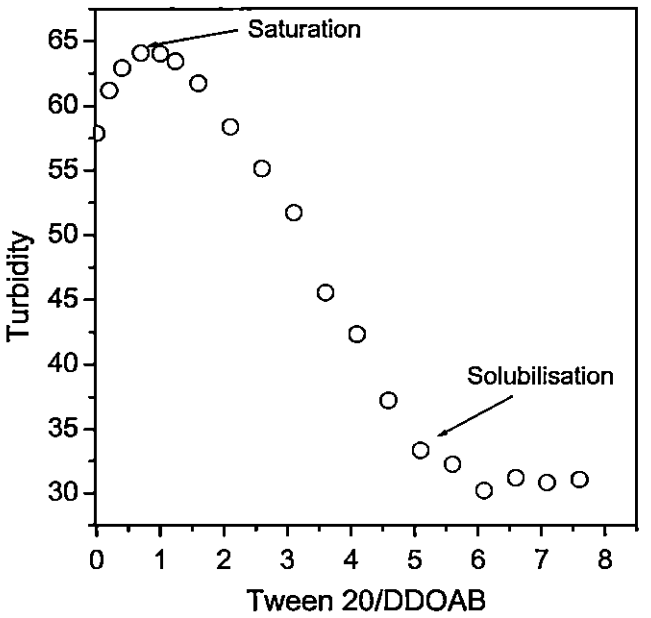

Figure 5.5. Turbidity at 300 nm as a function of Tween 20/DDOAB molar ratio at 25 °C

The microstructural transformation induced by the addition of Tween 20 to DDOAB vesicle dispersion is also investigated by DLS technique. Non sonicated aqueous DDOAB, at a concentration of 1.0 mM, is known to self-assemble into large unilamellar vesicles [5-9]. Based on an assumption of spherical vesicles, and the application of Stokes-Einstein equation, a hydrodynamic radius of ~324 nm is calculated for the neat DDOAB vesicle in the present experiment. This value is in close agreement with previously reported value of ~337 nm [53]. The vesicle size distribution of aqueous DDOAB in absence of Tween 20 surfactant is shown in figure 5.6 A. The plots of intensity against the average size (diameter) of DDOAB vesicles in presence at different Tween 20/DDOAB molar ratios are shown in figures 5.6 (B, C and D). Dramatic changes in the size could be observed with the addition of Tween 20. The values of the mean hydrodynamic radius (R_H) of the aggregates, monitored as a function of Tween 20/DDOAB molar ratios (based on an average of 15 measurements) along with the polydispersity index (PDI), are shown in table 5.1. Addition of Tween 20 at concentrations close to that of the observed saturation value in the turbidity measurement still produces a single peak in the DLS plot and causes the peak to shift to the right indicating an increase in the average hydrodynamic radius from ~324 nm to ~353 nm (figure 5.6 B). This corroborates our previous conclusion (from turbidity measurements) that the initial increase in the turbidity upto a mole ratio of 0.68 is due to the increase in the size of the vesicle as a result of the incorporation of Tween 20 monomers into the vesicle bilayer. The increase in the surface area due to Tween 20 incorporation in the vesicle accounts for the observed growth in size of the vesicle. Similar increment in the mean size of the phospholipids vesicle on the interaction with Polyoxyethylene glycol-12-acyloxystearates (PEG 1500-$C_{18}C_{12}$) surfactant has been recently reported by Thoren et. al. These authors have shown an increment in the hydrodynamic size of phospholipids vesicle from 45nm to 50nm at low concentration of PEG 1500- $C_{18}C_{12}$ surfactant [18]. When the Tween 20/DDOAB mole ratios were increased from 0.6 to 4.5, the present system showed a decrease in the mean size of the vesicle from ~353 nm to ~281 nm. This concentration condition (Tween 20/DDOAB molar ratio of 4.5) corresponds to the region where vesicle and micelles co-exist, i.e., between the saturation and solubilisation as per turbidity study. At Tween 20/DDOAB mole ratio of 6.0, the mean average size of

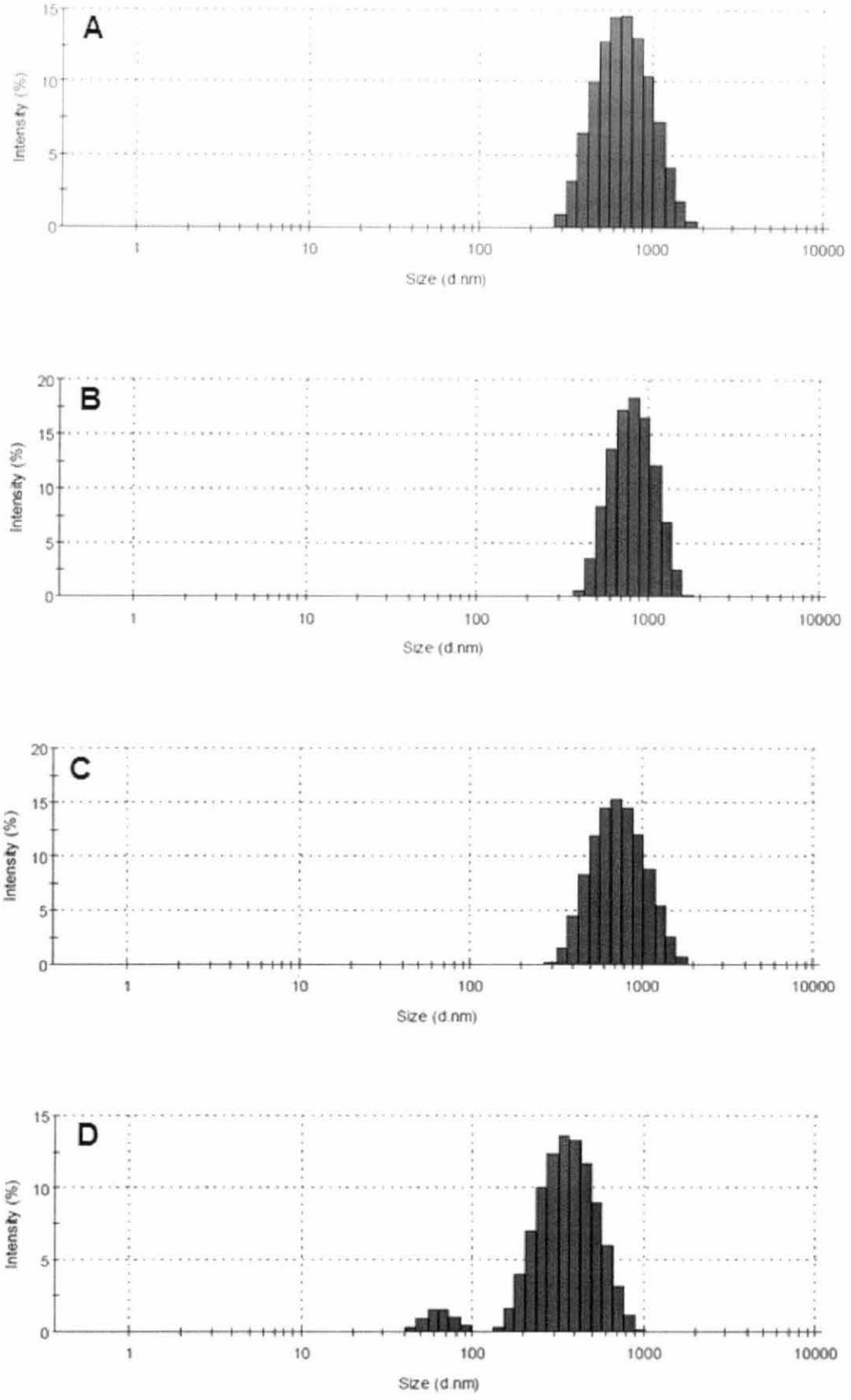

Figure 5.6. Size distribution of 1.0 mM DDOAB vesicle dispersion in absence of Tween 20 (A). (B), (C) and (D) correspond to Tween 20/DDOAB molar ratios of 0.6, 3.0 and 6.0 respectively.

Table 5.1. Results of Dynamic Light Scattering experiments for aqueous DDOAB and Tween 20/DDOAB systems at 25°C.

Systems	R_H (nm)	PDI
	337[a]	
Aqueous DDOAB (1 mM)	324	0.178
Tween 20/DDOAB = 0.6	353	0.174
Tween 20/DDOAB = 3.0	322	0.255
Tween 20/DDOAB = 4.5	281	0.291
Tween 20/DDOAB = 6.0	161	0.338

[a]as per reference 53.

the vesicle decreases to 161 nm and a new peak corresponding to a hydrodynamic radius of ~32 nm is observed (figure 5.6 D). This could be a region which indicates the presence of mixed micelles only. Without over-interpreting the DLS results and keeping the limitations of the technique in mind, the main conclusion can be drawn that the vesicle size is significantly influenced by the incorporation of Tween 20 to the vesicle dispersion.

5.4.1.3. Fluorescence Anisotropy Measurements

Anisotropy measurements are frequently used to study the properties and various interactions pertaining to the biological systems since it reveals the extent to which the probe motions are restricted by the anisotropic membrane environment [54]. In order to understand the changes induced on the vesicles of DDOAB, we measured the change in the steady-state fluorescence anisotropy of DPH in DDOAB dispersion as a function of Tween 20 concentration. The steady-state fluorescence anisotropy values (r) were calculated employing the equation [54]:

$$r = (I_{VV} - GI_{VH})/(I_{VV} + 2GI_{VH})$$

where I_{VV} and I_{VH} are the fluorescence intensities polarized parallel and perpendicular to the excitation light, and G (= I_{HV}/I_{HH}) is the instrumental grating factor. The anisotropy values were averaged over an integration time of 10s and maximum number of six measurements for each experimental run. The reason for using DPH is obvious; the change is more dramatic for DPH than for other molecules [54]. In the DSC experiment, the system is initially in the more ordered gel state and is transformed to a less ordered liquid crystalline state above the gel-to-liquid crystalline phase transition temperature. However, for turbidity measurements, the system as a whole remains in the more ordered gel state. Similar is the case with the anisotropy study. Hence the bulky DPH probe, which is localized in the deeper hydrophobic core region of the highly ordered DDOAB bilayer, display maximum anisotropy values at zero or in presence of low fraction of Tween 20.

Figure 5.7 shows the fluorescence anisotropy of DPH as a function of the Tween 20/DDOAB molar ratio. The anisotropy result depicts two critical points similar to that indicated by turbidity measurements, corresponding to saturation and solubilisation molar ratios (shown by arrows). The anisotropy value of the probe molecule for the lowest Tween 20/DDOAB molar ratio of 0.02 is much higher (~0.218) (as expected for lipids in a more ordered gel state below the T_m). The value remains almost steady upto molar ratio of 0.2, showing the restricted movement of the bulky DPH probe within the solid-like chain environment of the vesicle bilayer. However, as the disruption of the DDOAB bilayer is initiated, the anisotropy is lowered significantly until complete solubilisation by Tween-20 takes place. Once the solubilisation is completed at Tween 20/DDOAB molar ratio of 2.15, no further structural change occurs and hence no change in the fluorescence anisotropy of the probe molecule is brought about. Thus, the probe seems to be sensitive to the microstructural transitions taking place with the DDOAB vesicle. The values of saturation and solubilisation molar ratios obtained from the fluorescence anisotropic technique (~2.15) are lower than those from turbidity (4.0) and DSC (5.0) measurements. Since, DPH is a bulky probe with two strong hydrophobic aromatic rings, its incorporation would itself cause some bilayer defects as was observed with the benzene/phosphatidylcholine system,

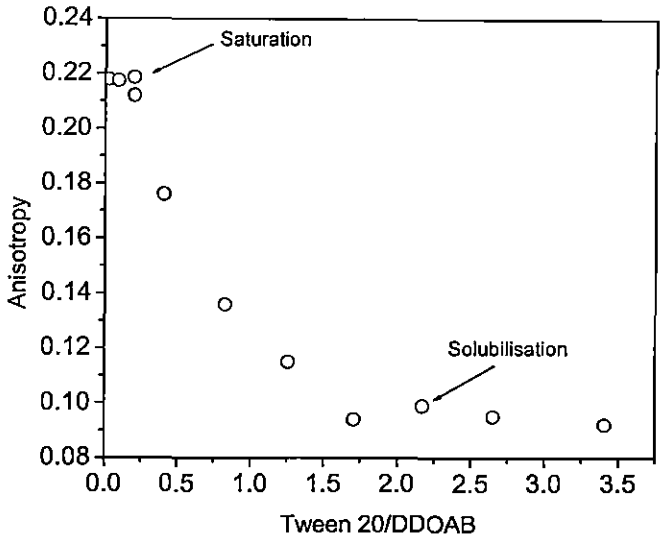

Figure 5.7. Steady-state anisotropy of DPH in Tween 20/DDOAB mixed systems at 25 °C.

at low benzene/lipid molar ratios [55]. The saturation and the rupture of the bilayer becomes even more easy by the addition of Tween 20 to the already perturbed vesicle structure. While the values of the saturation and solubilisation molar ratios from the fluorescence anisotropy method are less than those obtained from DSC and turbidity measurements, the results still correlate well with a solubilisation mechanism in which breaking down of the DDOAB vesicle structure and the formation of mixed micelles are dependent on the concentration of Tween 20 as suggested by Lichtenberg's three stage model.

5.4.2. Effect of quaternary cationics on the gel-to-liquid crystalline phase transition of DDOAB vesicle dispersion

On the addition of cationic alkyltrimethylammonium bromide surfactants (TTAB, CTAB and OTAB) to DDOAB dispersion, the gel-to-liquid crystalline phase transition temperature showed a complex behaviour depending on the hydrocarbon chain length of the surfactant. The changes are shown in figures 5.8 to 5.10. Surfactants having chain lengths shorter (TTAB and CTAB) than the vesicle

forming amphiphile (DDOAB) decrease the T_m whereas one having equal length (OTAB) elevates the T_m of aqueous DDOAB. In the concentration range studied (e.g., 0.5 mM to 3.0 mM), both depression and elevation in T_m is monotonous. Previously, it has been shown that the change in the T_m is a function of the length of the alkyl chain of the surfactant [29]. However, a careful analysis of the DSC thermograms of the present investigation shows that apart from the tail length, the concentration of alkyltrimethylammonium ions too plays a crucial role. The alkyl chain length and the concentration of the added surfactant affect not only the T_m of DDOAB vesicle but also the shape of the peak corresponding to the phase transition.

Figure 5.8 shows the DSC traces for 5.0 mM aqueous DDOAB dispersion in presence of various concentrations of TTAB. Addition of TTAB brings about a lowering of the T_m only, giving a single extrema (at the T_m) upto a concentration of 1.0 mM and no broadening or peak splitting is observed. Therefore, in the presence of TTAB upto 1.0 mM concentration, the chains become more mobile, the disorderness of the surfactant chains is increased, and thus the T_m is lowered. However, above 1.0 mM the peaks undergo broadening, i.e., the range of temperature of phase transition widens, and shows more than one extrema in the vicinity of the main T_m. This indicates that the mismatch in the tail length with that of the vesicle forming surfactants disrupts the stability of the vesicle only above 1.0 mM. This strongly suggests the presence of different kinds of domains within the vesicle. Some of these domains within the vesicle are rich in TTAB. This leads to vesicular patches of different sizes. The probable number of patches and hence the probable number of transitions at higher concentrations of surfactants can be examined and gives an idea about the distribution of the surfactants in the vesicle bilayer. A detailed theoretical analysis on the probable number of possible transitions have been performed by Kacperska [29]. The author found an increase in the number of independent transitions from 10 to 11 by an increase in the concentration of TTAB from 0.005 M to 0.0015 M. However, no particular trend could be observed in the changes of the independent transitions with the increase or decrease in the chain length of the added surfactant. Another important feature in the DSC thermogram of the DDOAB / TTAB mixture of the present study, is the

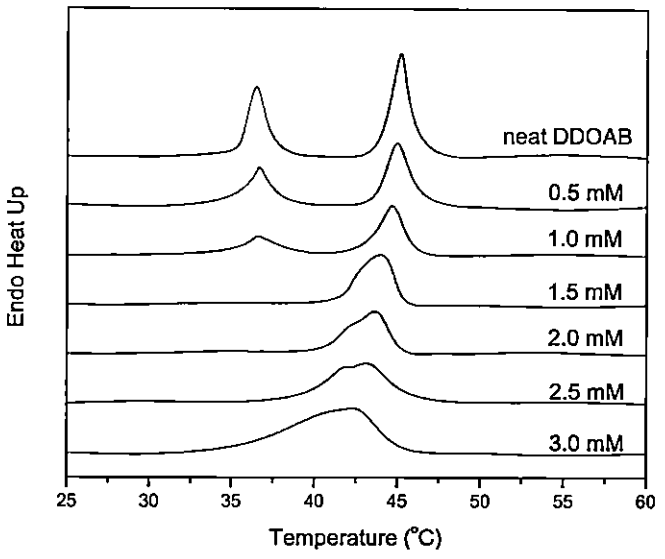

Figure 5.8. DSC upscans for 5.0 mM DDOAB dispersions in presence of TTAB. The concentrations of TTAB are indicated in the figure. Curves have been offset from each other to avoid overlap.

presence of the peak at 36°C upto 1 mM. As described earlier, this peak corresponds to the intervesicular interaction and is also called the pre-transition peak [30]. The retention of the pre-transition peak is a clear indication that the gel-to-liquid crystalline phase transformation is not direct, but passes via the pre-transition. Only above 1mM TTAB the phase transition becomes direct and is indicated by the disappearance of the pre-transition peak.

Figure 5.9 shows the DSC upscan thermograms for the 5 mM DDOAB in presence of various amounts of CTAB surfactant. The effect of adding 0.5 and 1.0 mM CTAB on the main T_m is similar as that produced by TTAB. At these concentrations the phase transition shifts to lower temperatures without any broadening in the width of the main peak, indicating little dependence of T_m on the vesicle curvature and structure [30]. Unlike TTAB, addition of CTAB even at the lowest concentration causes the pre-transition peak at 36°C to vanish as a result of decreased vesicle-vesicle interaction. Thus, the increase in the alkyl tail length of the cosurfactant from C_{14} to C_{16} leads to the insulation of the vesicle and hence prevents its aggregation in solution. Since the pre-transition peak disappears

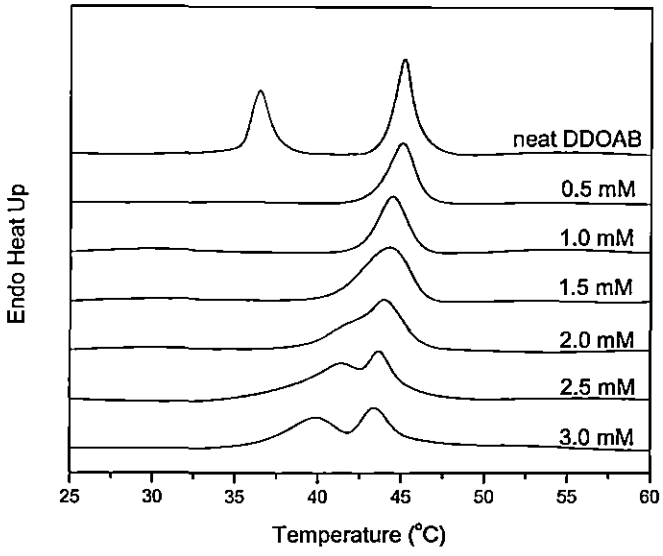

Figure 5.9. DSC upscans for 5.0 mM DDOAB dispersions in presence of CTAB. The concentrations of CTAB are indicated in the figure. Curves have been offset from each other to avoid overlap.

at the lowest CTAB concentration (0.5 mM), a direct gel-to-liquid crystalline phase transition can be predicted for this system. Presence of CTAB in excess of 1mM widens the main gel-to-liquid crystalline phase transition peak and in addition a new peak appears on the lower temperature side of the main peak. On further increasing the concentration of CTAB, the new peak becomes more pronounced while the intensity of the main peak decreases. In line with the findings of Feitosa, the presence of two pronounced transition peaks indicates presence of two differently populated vesicle, the difference being mainly in terms of the size and structure [56]. The peak at the lower temperature side of the thermogram represents the CTAB-rich vesicle while the peak corresponding to the main T_m represents the DDOAB-rich vesicle dispersion.

Figures 5.10 show the DSC thermograms of 1.0 mM DDOAB vesicles in water and in the presence of increasing amounts of OTAB. OTAB has the same hydrocarbon chain length (C_{18}) as that of the vesicle forming surfactant; DDOAB. Therefore, the question of mismatch of the tail does not arise for this system and the chains are expected to be less mobile within the vesicle. Thus it is expected that the disorderness decreases and consequently T_m increases as a function of OTAB

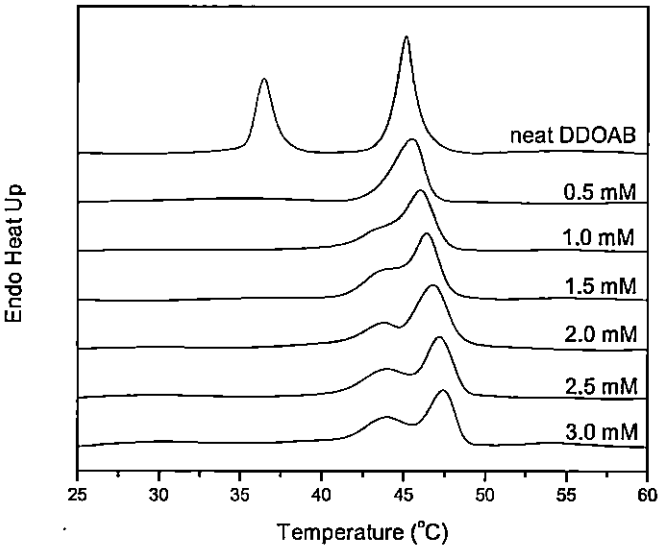

Figure 5.10. DSC upscans for 5.0 mM DDOAB dispersions in presence of OTAB. The concentrations of OTAB are indicated in the figure. Curves have been offset from each other to avoid overlap.

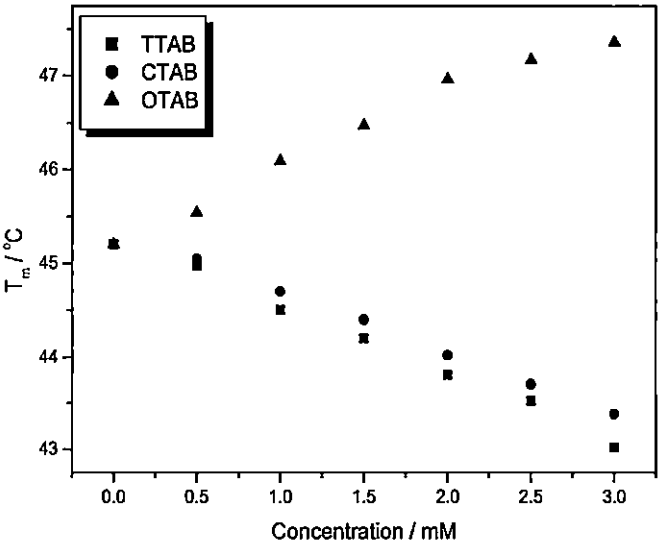

Figure 5.11. Variation of T_m of 5.0 mM DDOAB, the phase transition temperature, against concentration of added surfactants.

Table 5.2. Variation of the range and the main gel-to-liquid crystalline phase transition temperature of aqueous 5.0 mM DDOAB dispersion in presence of different alkyltrimethylammonium bromides.

Surfactant	Concentration (mM)	Range of T_m (°C)	Main T_m (°C)
	0.5	43.14-47.28	44.97
	1.0	42.58-46.49	44.51
TTAB	1.5	41.07-45.93	44.20
	2.0	39.95-46.01	43.82
	2.5	38.28-46.80	43.52
	3.0	34.78-47.12	43.02
	0.5	41.95-47.20	45.05
	1.0	40.99-47.04	44.41
CTAB	1.5	39.95-47.28	44.42
	2.0	38.76-47.52	44.02
	2.5	36.05-44.08	43.71
	3.0	34.38-48.80	43.38
	0.5	42.10-47.76	45.54
	1.0	40.75-48.48	46.09
OTAB	1.5	40.83-48.80	46.47
	2.0	40.43-50.23	46.96
	2.5	40.03-49.99	47.17
	3.0	40.03-49.67	47.36

concentration. As expected addition of OTAB to vesicle dispersion of DDOAB causes an increase in the T_m even at concentration as low as 0.5 mM. Therefore, we conclude that the incorporation of OTAB molecules inside the DDOAB vesicle is facile and increases the thermal stability of the vesicle dispersion even at low OTAB concentration. The other notable feature in the thermogram is the width of peak corresponding to the main T_m. Unlike TTAB and CTAB, addition of OTAB even in very small concentration (0.5 mM) widens the peak and it continues for the whole concentration range studied in the present investigation. Though there is an appearance of new peak on the low temperature side of the main T_m, the main T_m is always more pronounced than the new peak. This indicates that the system is rich in DDOAB vesicles at all concentrations of OTAB. The variation of T_m with concentration of different alkyltrimethylammonium bromide surfactants is shown in figure 5.11. The range of melting and the values for the main T_m of DDOAB in presence of various concentrations of TTAB, CTAB and OTAB are listed in table 5.2.

Although some reports on the interactions between alkyltrimethyl-ammonium bromides and synthetic vesicle formed by DDOAB are available in literature [29,30], the results are always not unambiguous and further study is necessary for a complete understanding of the subject. Therefore, we have re-examined the above mentioned aspects. However, the main aim of the present investigation is to examine the effect of some alkylpyridinium quaternary compounds on the T_m of DDOAB vesicles and to compare the results with that of the alkyltrimethylammonium counterpart having similar chain length. For this reason, CTAB and hexadecylpyridinium halides (Cl^- and Br^-) were chosen having equal tail length but with different head group geometry. The study should also highlight the effect of the counterions of the pyridinium head group (viz,. Cl^- and Br^-) on the phase transition of DDOAB vesicles. The non availability of literature on the interaction of CPB and CPC with DDOAB vesicles also prompted us for undertaking the present investigation.

The effect of CPC on the phase transition temperature of DDOAB vesicle is shown in figure 5.12. The change in T_m induced by the addition of CPC is small in the concentration range studied here, although the decreasing tendency of T_m is

intriguing. This is in contrast to the result observed in the case of alkyltrimethylammonium bromide/DDOAB systems, where a significant change (either increase or decrease) in T_m was observed at the same concentration range. Among the cationic surfactants, pyridinium compounds have smaller cmc's than that of the corresponding trimethylammonium compounds of similar hydrocarbon chain length. This may be due to the greater ease of packing the planar pyridinium group, compared to the tetrahedral trimethylammonium group into the vesicle [57]. The tetrahedral head group of CTAB, because of its geometry, would be expected to occupy greater space and push the vesicle head groups apart. This in turn would lead to a reduced head group interaction and ultimately disrupt the vesicle integrity, thus reducing the T_m to a greater extent. On the other hand, the planar pyridinium head groups of CPB or CPC would enter the vesicle with greater ease and may get sandwiched between the head groups of the bilayer, without disturbing either the T_m or the vesicle structure and also the curvature to any great extent. The DSC thermograms for CPB/DDOAB mixtures are shown in figure 5.13.

That the vesicle structure and curvature are little affected by penetration of CPB or CPC, is clearly seen from the width of the peaks corresponding to the main T_m. The width of the main T_m peak is rather narrow and remains the same for all concentrations of the additives. Thus, the conclusion that can be drawn from these observations is that the head group of the added cosurfactants, apart from the tail length, too play a major role in the stability of vesicle bilayers in aqueous solution. The range of melting and the values for the main T_m of DDOAB in presence of various concentrations of CPC and CPB are listed in table 5.3. When CTAB concentrations were above 2.0 mM, new peaks appeared on the low temperature side of the main T_m indicating the presence of different domains within the vesicle. However, additions of CPB and CPC at all concentrations show neither the emergence of new peaks nor a decrease in intensity of the phase transition peak. Hence, unlike the CTAB/DDOAB system, all patches inside the DDOAB vesicles consisting of CPB and CPC have identical composition. This would also mean that the hexadecylpyridinium/DDOAB systems consist of a single type of domain in which the melting takes place at a single temperature. The interaction of CPB and

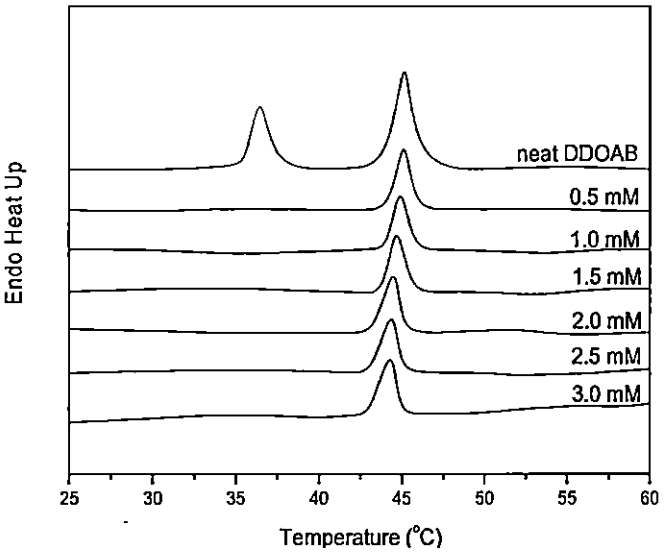

Figure 5.12. DSC upscans for 5.0 mM DDOAB dispersions in presence of CPC. The concentrations of CPC are indicated in the figure. Curves have been offset from each other to avoid overlap.

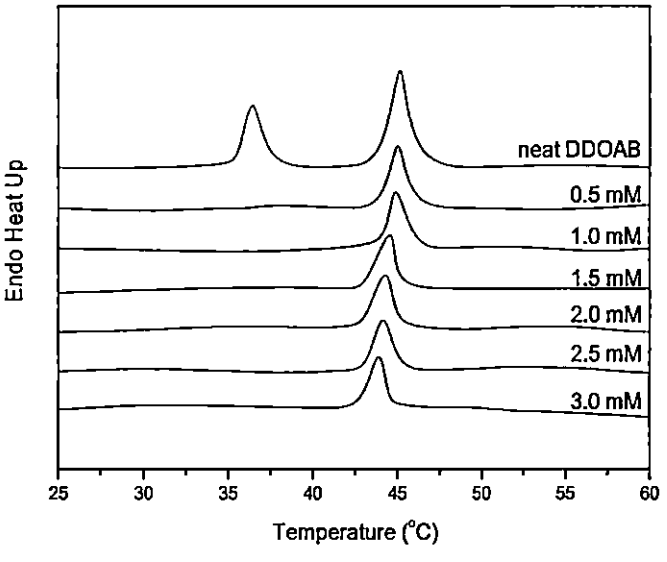

Figure 5.13. DSC upscans for 5.0 mM DDOAB dispersions in presence of CPB. The concentrations of CPB are indicated in the figure. Curves have been offset from each other to avoid overlap.

CPC with DDOAB also provides a route to study the effect of counterion of the cosurfactant on the T_m of DDOAB vesicles. Previously ithas been shown that NaCl raised whearas NaBr lowered the T_m of DDOAB. Thus, it would be interesting to check what happens when cosurfactants with different counterions are allowed to interact with DDOAB dispersion. Comparison of the results obtained from DSC measurements show that surfactant with the bromide counterion (CPB), decreases the gel-to-liquid crystalline phase transition temperature of DDOAB more than the one with chloride ion (CPC). The variation of T_m with surfactant concentration for CPB/DDOAB and CPC/DDOAB systems are shown in figure 5.14.

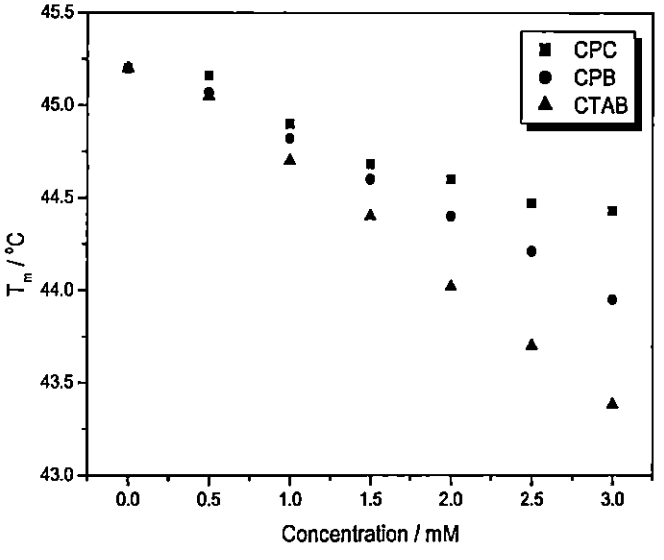

Figure 5.14. Variation of T_m of 5.0 mM DDOAB, the phase transition temperature, against concentration of added surfactants.

For the purpose of comparison, the values from CTAB/DDOAB systems are also included in the figure. The ionic radii of Cl^- and Br^- are 0.181 nm and 0.196 nm respectively [58]. Therefore, the charge on the more hydrated Cl^- is partially screened by the surrounding polar water molecules and these counterions are thus less effective in reducing the charge repulsion among the head groups of the vesicle. The Cl^- ions, therefore, cannot approach the highly charged surface of the vesicle as closely as the less hydrated Br^- ions. Therefore, it can neither screen the

charge at the surface of vesicles nor reduce the surface potential as effectively as the Br^- ions (less hydrated ions). The overall effect results in a less perturbed vesicle structure for the CPC/DDOAB system compared to CPB/DDOAB, and hence a smaller decrease in the T_m results.

Table 5.3. Variation of the range and the main gel-to-liquid crystalline phase transition temperature of aqueous 5.0 mM DDOAB in presence of varying concentrations of CPB and CPC

Surfactant	Concentration (mM)	Range of T_m (°C)	Main T_m (°C)
CPC	0.5	43.55-46.75	45.16
	1.0	43.35-46.48	44.91
	1.5	43.25-46.67	44.68
	2.0	42.38-46.19	44.60
	2.5	42.30-46.20	44.47
	3.0	42.07-45.58	44.43
CPB	0.5	42.72-47.16	45.07
	1.0	42.89-47.21	44.82
	1.5	42.21-46.61	44.60
	2.0	41.83-46.53	44.40
	2.5	41.35-46.27	44.21
	3.0	41.65-46.05	43.95

5.4.3. Effect of hydroxyaromatic compounds on the gel-to-liquid crystalline phase transition of DDOAB vesicle dispersion

In the previous chapter we have studied the effect of the hydroxyaromatic compounds, namely 1-naphthol, 2-naphthol, 2,3-dihydroxynaphthalene and 2,7-dihydroxynaphthalene on the microstructural transition of spherical micelles of cationic alkyltrimethylammonium bromide surfactants to long wormlike micelles and vesicles. In this section we have investigated the effect of the above named aromatic compounds in vesicular media of DDOAB, with special attention on the gel-to-liquid crystalline phase transition temperature of DDOAB vesicle dispersion.

Compared to cosurfactants, alkanes and alcohols, the literature on solubilization of aromatic molecules in bilayer membranes is very scarce. Simon and co-workers [59] described the effect of benzene on the thermal and structural properties of saturated phosphatidylcholine liposomes (1,2-distearoyl-phosphatidyl-choline and DPPC) for benzene/lipid ratios up to 9:1, and high lipid concentrations (30 % wt/wt) in water. At molar ratios lower than 1:1, there was an increase in the bilayer defects in the gel phase. Higher molar ratios (1:1 to 9:1) produced broad and multiple transitions. Freeze fracture and X-ray experiments show that benzene induces ripples in the fracture faces, modifies the lipid hydrocarbon packing, and increases the water spacing between bilayers in the gel state. At higher molar ratio (>9:1), benzene converts the multilamellar liposomes into smaller vesicles. From their partitioning study the same authors concluded that benzene was, on the average, partitioned in a nonpolar environment within the bilayer [60]. More recently, Bruockner and Rehage [61] investigated the solubilization of toluene in DMPC and DPPC giant vesicles by video-enhanced contrast microscopy and NMR. On the basis of morphological studies they could distinguish three domains of solubilization for toluene in DPPC giant vesicles: (1) At lower concentrations, i.e., at toluene/DPPC < 4.5, the vesicles kept their spherical shape. (2) In an intermediate range, 4.5:1 < toluene/DPPC < 18, shape fluctuations occurred, leading to nonspherical structures with low symmetry. Occasionally, lens-shaped occlusions of toluene within the membrane were detected. (3) Addition of even more toluene to the suspension induced the

formation of oil in water (o/w) emulsion in coexistence with vesicles. For DMPC, where the membrane is in a fluid state, a higher capacity of solubilization is reported. Recently, to elucidate the subtle interplay between morphology and bilayer properties, Jung et. al. have made a comparative study on the interaction of styrene with DDOAB vesicles [62]. These authors found that the solubilization of styrene in DODAB vesicles modulates the bilayer properties and hence their morphology.

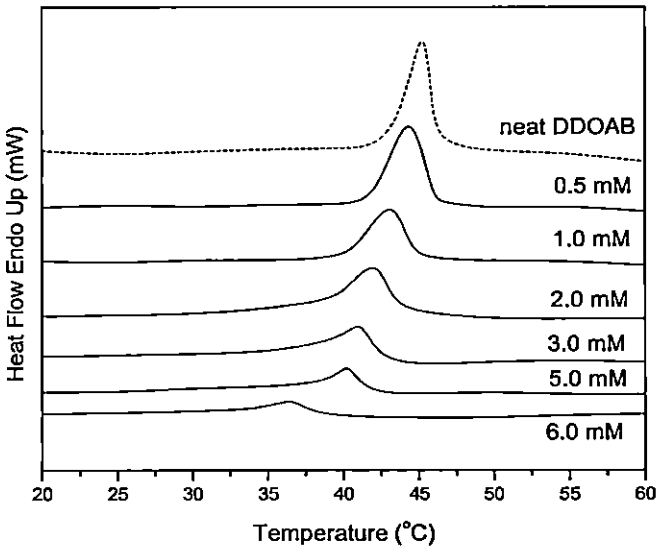

Figure 5.15. DSC upscans for 5.0 mM DDOAB dispersions in presence of varying concentrations of 1-naphthol. Curves have been offset from each other to avoid overlap.

Except for 2,7-dihydroxynaphthalene, all the other hydroxyaromatic compounds under investigation, are sparingly soluble in water. However, in vesicular DDOAB, the solubility of these compounds could be enhanced to as high as 6 mM. Therefore, systems comprising of these compounds (except 2,7 dihydroxy-naphthalene) could be studied only upto 6.0 mM. The effect of addition of 1-naphthol on the DSC thermal curves of DODAB vesicles is shown in Figure 5.15. The first thermograms in the figure (denoted by dotted line) correspond to pure 5.0 mM DODAB in water. In good agreement with previous reports [46, 47], well-defined peaks corresponding to the gel-to-liquid crystalline phase transition temperatures of 45.2 °C are obtained. Upon addition of 1- naphthol, a progressive

broadening of the main transition peak and a lowering of T_m is observed, indicating that the incorporation of 1-naphthol molecules in the DODAB bilayer has a disordering effect. Though broadening is observed with increasing concentrations, the peak does not disappear even when the 1-naphthol/DDOAB molar ratio exceeds unity. At this ratio the concentration of naphthol is the maximum (6.0 mM). This shows that the system is rich in vesicles even above 1:1 molar ratio and the naphthols just modify the structure and curvature of the vesicle. Hydroxyaromatic compounds like naphthols and their derivatives are fairly surface active and these compounds are expected to be embedded into micelles and vesicles strongly [63]. Therefore, the lowering of T_m of DDOAB vesicular dispersion results from the incorporation of the naphthol molecules into the bilayes and this subsequently decreases the thermal stability. Interestingly there is a substantial decrease in the main T_m value. This is in contrast with the case of addition of TTAB and CTAB additives in DDOAB vesicular dispersion, where a small decrease in the T_m was observed. For example, addition of 0.5 mM TTAB and CTAB causes a lowering in T_m from 45.2 °C to 44.97 °C and 45.05 °C respectively whereas, similar concentration of 1-naphthol causes a lowering in the T_m from 45.2°C to 44.3°C. Similar lowering was also observed for 2-naphthol and 2,3-dihydroxynaphthalene dopants as well. The presence of a single extrema in the thermograms for the hydroxyaromatic dopant-DDOAB systems suggests that all patches inside the vesicles have identical composition with similar intermolecular attractions. The sharp peaks observed for these systems are an indication that all the hydroxyaromatic dopant-DDOAB vesicle mixtures melt at the same temperature [64]. The effect of addition of 2-naphthol and 2,3-dihydroxynaphthalene on the DSC thermal curves of DODAB vesicles are shown in figure 5.16 and figure 5.17. While 1-naphthol, 2-naphthol and 2,3-dihydroxynaphthalene lower the T_m of DDOAB at all concentrations studied, the effect of 2,7-dihydroxynaphthalene on the thermal stability of DDOAB vesicle is quite interesting. Figure 5.18 shows the DSC thermograms of 5.0 mM aqueous DDOAB dispersion in absence and presence of different concentrations of 2,7-dihydroxynaphthalene. The nature of the DSC thermograms, on initial addition of 2,7-dihydroxynaphthalene to vesicular dispersion of DDOAB is very much similar to the changes brought about by 1- and 2- naphthol or 2,3-dihydroxynaphthalene.

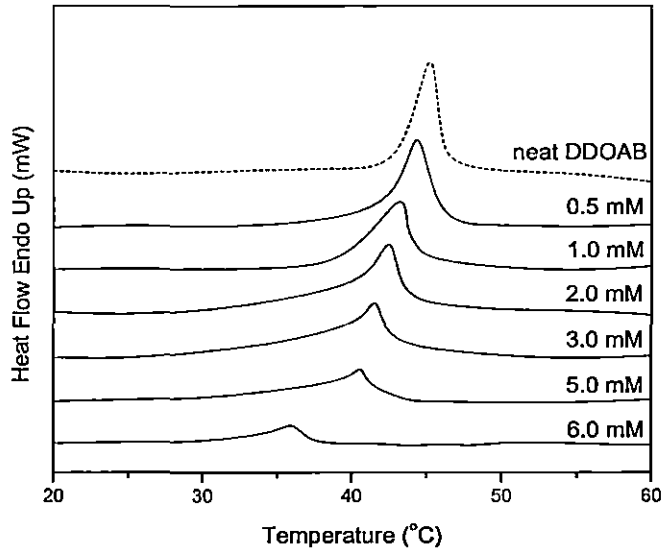

Figure 5.16. DSC upscans for 5.0 mM DDOAB dispersions in presence of varying concentrations of 2-naphthol. Curves have been offset from each other to avoid overlap.

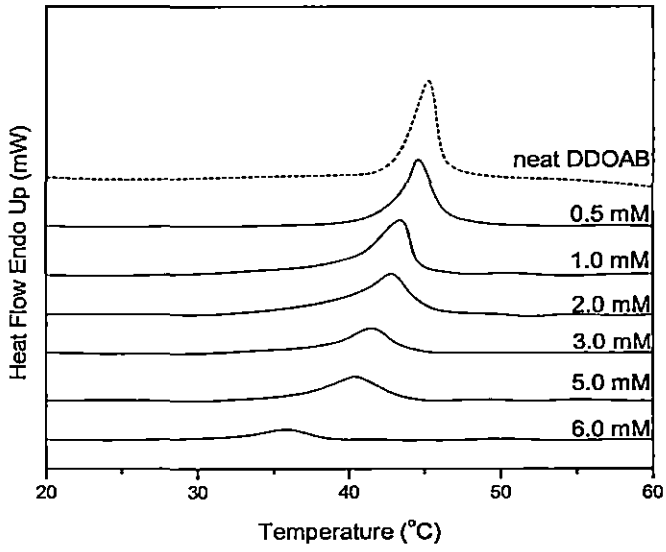

Figure 5.17. DSC upscans for 5.0 mM DDOAB dispersions in presence of varying concentrations of 2,3-dihydroxynaphthalene. Curves have been offset from each other to avoid overlap.

However, it is interesting to note that the decreasing trend of T_m with addition of 2,7-dihydroxynaphthalene is observed only upto a 2,7-dihydroxy-naphthalene/DDOAB mole ratio of 1:1, and above this ratio the transition temperature starts increasing (figure 5.18). The range of melting and the values for the main T_m of DDOAB in presence of various concentrations of dopants are listed in table 5.4.

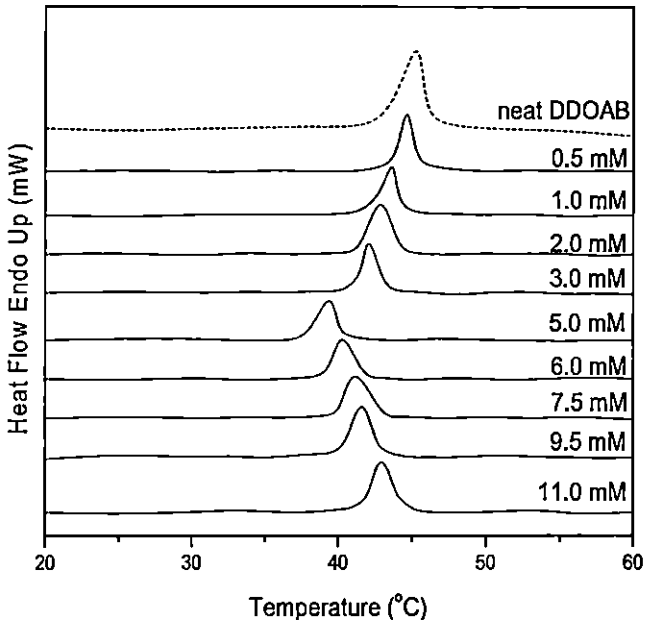

Figure 5.18. DSC upscans for 5.0 mM DDOAB dispersions in presence of varying concentrations of 2,7-dihydroxynaphthalene. Curves have been offset from each other to avoid overlap.

It has been seen that if the chain length of the cosurfactant molecule or the hydrophobic part of the organic additive match the tail length of the vesicle, the vesicle chain is expected to be less mobile and the disorderness is considerably decreased. This ultimately leads to the increase in the T_m value. On the other hand, mismatching of the vesicle tail length with that of the additive molecules disrupt the stability of the vesicle. This results in the formation of different types of domain within the vesicle; some are rich in additive molecules and some in vesicle forming amphiphilic molecules. Ultimately, the stability of the vesicle decreases.

Table 5.4. Variation of the range and the main gel-to-liquid crystalline phase transition tempera-ture of aqueous 5.0 mM DDOAB dispersion in presence of hydroxy aromatic dopants.

Dopant	Concentration (mM)	Range of T_m (°C)	Main T_m (°C)
	0.5	40.21-47.40	44.30
	1.0	37.45-46.34	43.08
	2.0	37.12-45.44	41.95
1-naphthol	3.0	37.05-44.32	41.03
	5.0	34.34-43.09	40.22
	6.0	31.37-42.36	36.41
	0.5	38.88-48.02	44.32
	1.0	37.23-46.58	43.29
2-naphthol	2.0	36.61-45.55	42.47
	3.0	35.38-45.44	41.56
	5.0	33.53-44.42	40.62
	6.0	30.55-38.77	35.91
	0.5	39.28-48.84	44.53
	1.0	37.44-47.20	43.39
2,3-Dihydroxynaphthalene	2.0	37.02-46.37	42.89
	3.0	34.97-44.83	41.44
	5.0	33.84-44.63	40.42
	6.0	30.76-39.79	35.79
	0.5	41.65-47.00	44.63
	1.0	40.11-45.66	43.60
	2.0	40.52-45.14	42.88
	3.0	39.90-44.73	42.06
2,7-Dihydroxynaphthalene	5.0	37.02-41.75	39.39
	6.0	38.05-42.88	40.31
	7.5	39.18-43.50	41.13
	9.5	39.39-44.63	41.55
	11.0	39.79-46.07	42.99

The initial lowering of T_m for the 2, 7- dihydroxynaphthalene - DDOAB vesicular system upto the mole ratio of 1:1, undoubtly point out to the result of mismatch of the surfactant tail length with the molecular length of the dopant molecule. The destabilisation of the vesicle is brought about in the presence of hydroxyaromatic compounds, the length of which is less than that of DDOAB molecules. Density Functional Theory (DFT) calculations (B3LYP) with 6-31 G Basic set shows that DDOAB has a molecular length of ~21.8 A°. On the other hand, the molecular length of 2,7-dihydroxynaphthalene is ~8 A°. This clearly supports the above argument. Dihydroxynaphthalene derivatives are embedded even more strongly in DDOAB than in micelles of CTAB. It is reasonable to argue that the orientation of the dihydroxynaphthalene is such that one OH group is buried inside the hydrocarbon core of the outer layer of the vesicle. Much shorter molecular size of the additive leads to disruption of the vesicle and consequently the T_m is decreased. However, as the concentration of the additive is increased above 1:1 mole ratio, the additive molecules viz., 2,7-dihydroxynaphthalene are buried deep inside the hydrocarbon tail region and in all probabilities form head-to-tail dimers via hydrogen bonding interaction with the already embedded unimers. DFT study confirms the H-bond formation between the dopant pair in hydrocarbon solvent. Considering the hydrogen bond length alongwith the molecular lengths of 2,7-dihydroxynaphthalene, it seems that the dimer length is now some what closer to the length of the hydrocarbon chain of DDOAB (DFT calculation as above shows that the dimers of 2,7-dihydroxynaphthalene is ~17.4 A°). This means that the addition of 2,7-dihydroxynaphthalene above 1:1 mole ratio, increases the stability of the vesicle and hence T_m is increased to a considerable extent because under this condition the length of the dimer of the additive is more closer to the lengths of the vesicle forming surfactant chain.

References

1. Engberts JBFN, Hoekstra D: *Biochim Biophys Acta* 1996, 1241:323-340.
2. Lasic,D.D. *Liposomes. From Physics to Applications;* Elsevier: Amsterdam,1993
3. Fendler, J.; H. *Membrane Mimetic Chemistry;* Wiley-Interscience: New York, 1982
4. Carmona-Ribeiro, A. M. *Chem. Soc. Rev.* **1992**, 21, 209.
5. Cuccovia, I. M.; Feitosa, E.; Chaimovich, H.; Sepulveda, L.; Reed, W. Size, *J. Phys. Chem.* **1990**, 94, 3722.
6. Feitosa, E.; Brown, W. *Langmuir* **1997**, 13, 4810.
7. Cuccovia, I. M.; Sesso, A.; Abuin, E.; Okino, P. F.; Tavares, P. G.; Campos, J. F. S.; Florenzano, F. H.; Chaimovich, H. *J. Mol. Liquids* **1997**, 72, 323.
8. Blandamer, M. J.; Briggs, B.; Cullis, P. M.; Kacperska, A.; Engberts, J. B. F. N.; Hoekstra, D. *J. Indian Chem. Soc.* **1993**, 70, 347.
9. Kunitake, T.; Okahata, Y. *J.Am.Chem.Soc* **1977**, 99, 3860.
10. Carmona-Rebeiro, A.M.; Chaimovich, H. *Biochem. Biophys.Acta*, **1983**, 733, 172.
11. Lichtenberg, D.; Robson, R. J.; Dennis, E. A. *Biochim. Biophys. Acta* **1983**, *737*, 285.
12. Lichtenberg, D. *Biochim. Biophys. Acta* **1985**, 821, 470.
13. Paternostre, M.T.; Roux, M.; Rigaud, J.-L. *Biochemistry* **1988**, 27, 2668.
14. Edwards, K.; Almgren, M.; Bellare, J.; Brown W. *Langmuir* **1989**, 5, 473.
15. Vinson, P.K.; Talmon, Y.; Walter, A. *Biophys. J.* **1989**, 56, 669.
16. Edwards, K.; Almgren, M. *J. Colloid Interf. Sci.* **1991**, 147, 1.
17. Lehninger, A. L.; Nelson D L, Cox, M. M. *Principles of Biochemistry.* 2nd Ed. Worth Publishers Inc. New York. 2000
18. Thoren, P. G.; Soderman, O.; Engstrom, S.; Corswant, C. *Langmuir* **2007**, 23, 6956
19. Johnsson, M.; Edwards, K. *Langmuir* **2000**, 16, 8632.
20. Almgren, M. *Biochim. Biophys. Acta* **2000**, 1508, 146.
21. Edwards, K.; Almgren, M. *Prog. Colloid Polym. Sci.* **1990**, *82*, 190.
22. Feitosa, E.; Barreleiro, P. C. A. *Prog. Colloid Polym. Sci.* **2004**, 128, 163.
23. Silvander, M.; Karlsson, G.; Edwards, K.; *J. Colloi Interface Sci.* **1996**, 179, 104

24. De La Maza, Parra, J.L. *Colloid Polym Sci* **1996**, 274, 253
25. Seras, M.; Edwards, K.; Almgren, M.; Carlson, G.; Ollivon, M.; Lesieur, S. *Langmuir*, **1996**, 12, 330
26. Feitosa, N.M.; Bonassi,W. Loh, Langmuir 22 (2006) 4512.
27. Cocquyt, J.; Olsson, U.; Olofsson, G.; Van der Meeren, P. *Langmuir* **2004**, 20, 3906.
28. Barreleiro, P.C.A.; Olofsson, G.; Brown, W.; Edwards, K.; Bonassi, N.M.; Feitosa, E. *Langmuir* **2002**, 18, 1024.
29. Kacperska, A. *J. Thermochem. Anal.* **1995**, 45, 703.
30. Alves, F.R.; Zaniquelli, M.E.D.; Loh, W.; Castanheira, E.M.S.; Real Oliveira, M.E.C.D.; Feitosa, E. *J. Colloid Interf. Sci.* **2007**, 316, 132.
31. Blandamer, M. J.; Briggs, B.; Cullis, P. M.; Engberts, J. B. F. N.; Kacperska, A. *J. chem.. Soc. Faraday Trans.* **1995**, 91, 4275
32. Alves, F. R.; Feitosa, E. *Thermochimica Acta* **2008**, 472, 41
33. Umemura, J.; Kawai, T.; Takenaka, T.; Kodama, M.; Ogawa, Y.; Seki, S. *Mol. Cryst. Liq. Cryst.* **1984**,112, 293.
34. Laughlin, R.G. *The Aqueous Phase Behavior of Surfactants*. Academic Press, London, p. 29. 1994.
35. Kunieda, H.; Shinoda, K. *J. Phys. Chem* **1978**, 82, 1710.
36. Fendler, J.H. *Membrane Mimetic Chemistry;* Wiley-Interscience: New York, 1982.
37. Carmona-Ribeiro, A.M. *Chem. Soc. Rev.* **1992**, 21, 209.
38. Feitosa, E.; Brown, W. *Langmuir* **1997**, 13, 4810.
39. Feitosa, E.; Barreleiro, P.C.A.; Olofsson, G. *Chem. Phys. Lipids* **2000**, 105, 201.
40. Cocquyt, J.; Olsson, U.; Olofsson, G.; Van der Meeren, P. *Langmuir* **2004**, 20, 3906
41. Kodama, M.; Kunitake, T.; Seki, S. *J. Phys. Chem* **1990**, 94, 1550.
42. Linseisen, F. M.; Bayerl, S.; Bayerl, T. M. *Chem. Phys. Lipids* **1996**, 83, 9.
43. Schulz, P. L.; Rodriguez, J. L.; Soltero-Martinez, F. A.; Puig, J. E.; Proverbio, Z. E. *J. Therm. Anal.* **1998**, 51, 49.
44. Feitosa, E.; Barreleiro, P. C. A.; Olofsson, G. *Chem. Phys. Lipids* **2000**, 105, 201
45. Alves, F. R.; Feitosa, E. *Thermochim. Acta* **2008**, 472, 41

46. Blandamer, M. J. Briggs, B. Cullis, P. M. Engberts, J. B. E. N.; Kaeperska, A. *J. Chem. Soc. Faraday Trans* **1995**, 91, 4275.

47. Kacperska, A. *J.Therm.Anal.* **1995**, 45, 703

48. Blandamer, M. J.; Briggs, B.; Cullis, P. M.; Engberts, J. B. F. N.; Wagenaar, A.; Smits, E.; Hoekstra, D.; Kacperska, A. *J. Chem. Soc., Faraday Trans.* **1994**, 90, 2709.

49. Rand, R. P.; Chapman, D.; Larsson, K.; *Biophys. J.* **1975**, 15, 1117.

50. Janiak, M. J.; Small, D. M.; Shipley, G. G. *Biochemistry* **1976**, 15, 4575.

51. Barreleiro, P. C. A.; Olofsson, G.; Brown, W.; Edwards, K.; Bonassi, N. M.; Feitosa, E. *Langmuir* **2002**, 18, 1024

52. Silvander, M.; Karlsson, G.; Edwards, K. *J. Colloi Interface Sci.* **1996**, 179, 104

53. Feitosa, E.; Alves, F. R.; Niemiec, A.; Real Oliveira, M. E. C. D.; Castanheira, E. M. S.; Baptisa, A. L. F. *Langmuir* **2006**, 22, 3579

54. Lakowicz, J.; *Principles of fluorescence Spectroscopy*, Plenum Press, New York, 1983

55. McDaniel, R. V.; Simon, S. A.; McIntosh, T. J.; Borovyagin, V. *Biochemistry* **1982**, 21, 4116.

56. Feitosa, E.; Karlsson, G.; Edwards, E. *Chem. Phys. Lipids* **2006**, 140, 4810

57. Rosen, M.J.; *Surfactants and Interfacial Phenomena*; Wiley-Interscience: New York, 2004.

58. Barthel, J.; Krienke, H.; Kunz, W. *Physical Chemistry of Electrolyte Solutions – Modern Aspects*, Steinkopf/Springer, Darmstadt/New York, 1998.

59. McDaniel, R. V.; Simon, S. A.; McIntosh, T. J.; Borovyagin, V. *Biochemistry* **1982**, 21, 4116.

60. Simon, S. A.; McDaniel, R. V.; McIntosh, T. J. *J. Phys. Chem.* **1982**, 86, 1449.

61. Bruockner, E.; Rehage, H. *Prog. Colloid Polym. Sci.* **1998**, 109, 21.

62. Jung, M.; Hubert, D. H. W.; Veldhoven, E.; Frederik, P. M.; Blandamer, M. J.; Briggs, B.; Visser, A. J. W. G.; Herk, A. M.; German, A. L.; *Langmuir* **2000**, 16, 968.

63. Ali, M.; Jha, M.; Das, S. K.; Saha, S. K.; *J. Phys. Chem. B* **2009**, 113, 15563.

64. Shapovalov, V.; Tronin, A. *Langmuir* **1997**, 13, 4870.